

Cooperative OFDM with Amplify-and-Forward Relaying with Timing Offset

K. Raghunath and A. Chockalingam

Department of ECE, Indian Institute of Science, Bangalore 560012, INDIA

Abstract—In this paper, we investigate cooperative OFDM communications using amplify-and-forward (AF) protocol at the relays, in the presence of imperfect timing synchronization. In most studies on cooperative communications, perfect time synchronization among cooperating nodes is assumed. In practice, however, due to imperfect time synchronization, orthogonality among the subcarriers of the different nodes' signals at the destination receiver can be lost, causing inter-symbol interference (ISI). In this paper, we derive analytical expressions for the average SINR at the DFT output at the destination as a function of timing offset in cooperative OFDM with AF protocol, and illustrate the SINR degradation as a function of the timing offset. We also present an interference canceling (IC) receiver to mitigate the effects of ISI when there is timing offset. We show that the proposed IC receiver achieves improved BER performance even when timing offsets are large.

I. INTRODUCTION

Cooperative communications have become popular because of the diversity benefit they can provide to single-antenna communication terminals [1]. OFDM is popular because of its bandwidth efficiency without requiring equalization at the receiver [2]. With an intent to achieve the benefits of both cooperation as well as OFDM, cooperative OFDM networks have been increasingly investigated [3]-[8]. In [3],[4] Gui and Cimini Jr devise bit loading algorithms for cooperative OFDM systems with decode-and-forward (DF) relaying, considering a single source-destination pair and multiple cooperating relays. In [5], they propose an OFDM-based selective relaying scheme in a multihop cooperative network, where the relay selection at each hop is performed on a per-subcarrier basis and joint selection is adopted at the last two hops. In [6], Jamshidi *et al* derive exact expression and tight lower bound for the outage probability of space-frequency coded cooperative OFDM system. Effect of carrier frequency offsets on the relay-to-destination links in cooperative OFDM is investigated in [7]. In [8], interference mitigation techniques to alleviate the effect of inter-symbol interference (ISI) and inter-carrier interference (ICI) caused due to frequency selectivity of the channel and violation of 'quasi-static' assumption in space-frequency block coded cooperative OFDM are presented and analyzed for amplify-and-forward (AF) and decode-and-forward (DF) relaying.

Most of the above studies on cooperative OFDM assume perfect timing synchronization among various nodes. However, due to imperfect time synchronization, orthogonality among different nodes' signals at the destination receiver can be lost, causing ISI. In cooperative networks without OFDM this issue of timing errors has been investigated in [9]-[10]. But the

This work was supported in part by the DRDO-IISc Program on Advanced Research in Mathematical Engineering.

issue of *timing offsets in cooperative OFDM* (due to imperfect time synchronization) has not been adequately addressed in the literature so far. Accordingly, our focus in this paper is to investigate the effect of timing offsets on the performance of cooperative OFDM and the associated ISI mitigation techniques. We consider AF relaying since it has the advantage of low implementation complexity and simplicity compared to the DF relaying. Our contributions in this paper include: *i*) we analytically characterize the interference caused due to timing offsets in cooperative OFDM with AF relaying; we quantify the degradation in the SINR at the DFT output at the destination receiver as a function of non-zero timing offset, and *ii*) using the interference characterization, we present an interference mitigation receiver to improve the performance in cooperative OFDM even when timing offsets are large.

II. SYSTEM MODEL

Consider a three-node cooperative OFDM network with a source (*S*), relay (*R*), and destination (*D*). The *S*-to-*D*, *S*-to-*R*, and *R*-to-*D* links are assumed to be Rayleigh faded and frequency selective with delay spreads $L_1 - 1$, $L_2 - 1$, and $L_3 - 1$, respectively. Let $h_d[n]$, $h_s[n]$ and $h_r[n]$ denote the channel impulse response (CIR) of the *S*-to-*D*, *S*-to-*R* and *R*-to-*D* links, respectively. Assume that there are N OFDM subcarriers. In the 1st time slot (*broadcast phase*), *S* transmits one OFDM frame of duration $(N + N_g)T_s$, where T_s is one sample time and N_g is the cyclic prefix (CP) length. The minimum CP length required is $\max(L_1 - 1, L_2 + L_3 - 2)$. The transmitted OFDM frame consisting of data symbols $X[k]$, $0 \leq k \leq N - 1$, is given by

$$x[n] = \frac{1}{N} \sum_{k=0}^{N-1} X[k] e^{i \frac{2\pi n k}{N}}, \quad -N_g \leq n \leq N - 1. \quad (1)$$

Both *R* and *D* receive this OFDM frame. The received signal at *D* and *R*, denoted by $y_d[n]$ and $y_r[n]$, respectively, are

$$y_d[n] = h_d[n] * x[n] + z_1[n], \quad (2)$$

and

$$y_r[n] = h_s[n] * x[n] + z_2[n], \quad (3)$$

where $*$ indicates linear convolution, and $z_1[n]$ and $z_2[n]$ denote AWGN terms at *D* and *R*, respectively, in the 1st time slot with variance N_0 . In the 2nd time slot (*relaying phase*), *R* amplifies its received signal by gain G and transmits it. The received signal at *D* in two time slots is

$$y(n) = \underbrace{h_d[n] * x[n] + z_1[n]}_{\text{Rx signal in time slot 1}} + \underbrace{G h_r[n] * h_s[n] * x[n] + G h_r[n] * z_2[n] + z_3[n]}_{\text{Rx signal in time slot 2}}, \quad (4)$$

where $z_3[n]$ denotes the AWGN with variance N_0 at D in the 2nd time slot.

In case of perfect time alignment, the input to the DFT unit of the receiver at D during 1st time slot is

$$y_d[n] = h_d[n] \star x[n] + z_1[n], \quad (5)$$

where \star indicates circular convolution, and the corresponding output on the k th subcarrier is given by

$$Y_d[k] = H_d[k]X[k] + Z_1[k], \quad (6)$$

where $H_d[k]$ is N -point DFT of $h_d[n]$. The input to the DFT unit during the 2nd time slot is given by

$$y_r[n] = Gh_s[n] \star h_r[n] \star x[n] + h_r[n] \star z_2[n] + z_3[n], \quad (7)$$

and the corresponding output on the k th subcarrier carrier is

$$Y_r[k] = GH_1[k]H_2[k]X[k] + GH_2[k]Z_2[k] + Z_3[k], \quad (8)$$

where $H_1[k]$ and $H_2[k]$ are N -point DFTs of $h_s[n]$ and $h_r[n]$, respectively, and $Z_2[k]$ and $Z_3[k]$ are the noise components at the DFT output due to $z_2[n]$ and $z_3[n]$, respectively.

III. EFFECT OF TIMING OFFSET ON OUTPUT SINR

In this section, we analytically characterize the various interference terms at the DFT output caused by imperfect timing alignment at D . Let μ denote the timing offset at D with respect to perfect timing, in number of samples. Figure 1 shows the frame timing and processing windows at D without and with timing offset. The processing window without timing offset in Fig. 1 corresponds to the ideal processing window, i.e., $\mu = 0$. For $\mu \neq 0$, depending on whether $\mu > 0$ or $\mu < 0$, interference from either next frame (NF), which we refer to as ISI-NF (Inter-Symbol Interference from Next frame) or previous frame (PF), which we refer to as ISI-PF (Inter-Symbol Interference from Previous frame) results. Apart from this, due to the loss of some samples in some or all of the frames, interference from the carriers of the present frame also occurs, which we refer to as ISI-CF (Current Frame Self Interference). In the following, assuming that all links have the same delay spread L , we derive the expressions for the DFT output on the k th subcarrier in times slots 1 and 2. To do this, six different cases of timing offset (referred to as **Cases a to f**), depending on the value of μ , need to be considered. Let W_1 and W_2 denote the processing windows at D for the signal from S to D and R to D , respectively. Also, define

$$\rho_{qk}(n_a, n_b) \triangleq \frac{1}{N} \sum_{n=n_a}^{n_b} e^{\frac{i2\pi n(q-k)}{N}}. \quad (9)$$

Case a): $0 < \mu \leq L - 1$. In this case, within W_1 , there will be *i*) a loss of $\mu - j$ samples in the frame arriving through j th path of the link from S to D for $j < \mu$, and *ii*) $\mu - j - l$ samples of the frames arriving at the destination through j th path from S to R and then through l th path from R to D for $l + j < \mu$ causing ISI-CF. The output of DFT-1¹ on the k th subcarrier, and the average power in each of the desired signal (DS) and interference terms are given in Table-I, where

¹Henceforth, we refer to the DFT in 1st and 2nd time slots as DFT-1 and DFT-2, respectively.

$$(n_1, n_2) = \begin{cases} (0, N - 1 - \mu + j), & \text{for } 0 \leq j < \mu \\ (0, N - 1), & \text{for } j \geq \mu, \end{cases} \quad (10)$$

$$(n_3, n_4) = (N - \mu + j + l, N - 1). \quad (11)$$

Also, within W_2 , there will be *i*) a loss of $\mu - j - l$ samples of the frames arriving at the destination through j th path of the link from S to R and then through l th path of the link from R to D for $l + j < \mu$ causing ISI-CF, and *ii*) $\mu - j$ samples of the next frame, coming to the receiver through the direct path for $j < \mu$ causing ISI-NF. The output of DFT-2 on the k th carrier, and the corresponding average powers in each term are given in the Table-2, where

$$(n_1, n_2) = \begin{cases} (0, N - 1 - \mu + j + l), & \text{for } j + l < \mu \\ (0, N - 1), & \text{for } j \geq \mu, \end{cases} \quad (12)$$

$$(n_3, n_4) = (N - \mu + j, N - 1), \quad (13)$$

In Table-I, $X_f[n]$ denotes the symbols in the next frame, and h_{df} denotes the CIR of the S -to- D link during the next frame.

Case b): $L - 1 < \mu \leq N_g$. In this case, in W_1 , the expressions for the output of DFT-1 on the k th subcarrier and the average powers can be obtained from the expressions for *Case a*) given in Table-I by using

$$(n_1, n_2) = (0, N - 1 - \mu + j), \quad \forall j \quad (14)$$

and (n_3, n_4) as given in (11). The expressions in W_2 in this case are the same as the corresponding expressions for *Case a*), but without the condition $j < \mu$ in the ISI-NF term.

Case c): $\mu > N_g$. The expressions in W_1 in this case are same as those of *Case a*) in Table-I, with (n_1, n_2) given by (14) and without the condition $j + l < \mu$ in the ISI-CF term. Also, the expressions in W_2 in this case are same as those of *Case a*), without the conditions on j and $j + l$ and with

$$(n_1, n_2) = (0, N - 1 + l + j + \mu), \quad (15)$$

$$(n_3, n_4) = (N - \mu + j, N - 1). \quad (16)$$

Case d): $0 < -\mu \leq L - 1$. In this case, within W_1 , there will be, *i*) circularly shifted versions of the frame arriving through the direct path, causing no loss of orthogonality, and *ii*) $j + l - \mu - N_g$ samples of the previous frames for $l + j > N_g + \mu$, arriving at the destination through j th path from S to R and then through l th path from R to D , causing ISI-PF. The expressions for the DFT-1 output and the average powers for this case are given in the Table-I, where $X_p[n]$ denotes the symbols in the previous frame passing through CIRs h_{sp} and h_{rp} on the S -to- R and R -to- D links, respectively, and

$$(n_1, n_2) = (0, j + l - \mu - N_g - 1). \quad (17)$$

Also, within W_2 , there will be a loss of $j + l - \mu - N_g$ samples of the frames arriving at D through j th path from S to R and then through l th path from R to D for $l + j < \mu$, causing ISI-CF. The corresponding expressions are in Table-I, where

$$(n_1, n_2) = \begin{cases} (0, N - 1), & \text{for } j + l \leq N_g + \mu, \\ (l + j - \mu - N_g, N - 1), & \text{for } j + l > N_g + \mu. \end{cases} \quad (18)$$

Case e): $L - 1 < -\mu \leq N_g$. In this case, within W_1 , there will be *i*) circularly shifted version of the frame arriving through the direct path causing no loss of orthogonality for

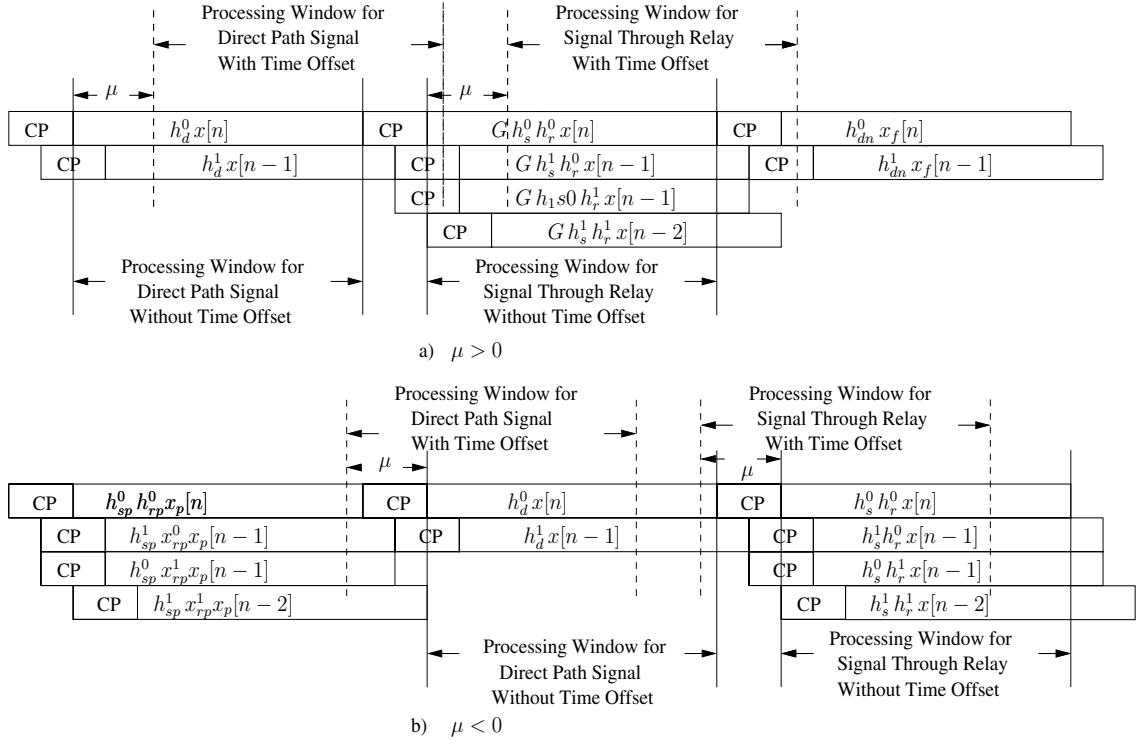


Fig. 1. Different timing misalignment scenarios for $\mu > 0$ and $\mu < 0$ for $L = 2$.

$j \leq N_g + \mu$, and there will be a loss of $j - \mu - N_g$ samples of the frame coming through the direct path for $j > N_g + \mu$ causing ISI-CF, and *ii*) $l + j - \mu - N_g$ samples of the previous frame arriving at the destination through j th path from S to R and then through l th path from R to D for $l + j > N_g + \mu$ causing ISI-PF. The corresponding expressions for this case are given in the Table-I, where

$$(n_1, n_2) = \begin{cases} (0, N - 1), & \text{for } j \leq N_g + \mu \\ (j - \mu - N_g, N - 1), & \text{for } j > N_g + \mu, \end{cases} \quad (19)$$

$$(n_3, n_4) = (0, l + j - \mu - N_g - 1), \quad (20)$$

In this case, within W_2 , there will be *i*) circularly shifted versions of the frame through relay for $l + j \leq N_g + \mu$, and there will be a loss of $j + l - \mu - N_g$ samples of the frames arriving at the destination through $l + j$ th path through the relay causing ISI-CF, and *ii*) $j - N_g - \mu$ samples of the present frame coming through the direct path for $j > N_g + \mu$ causing ISI-CF. The corresponding expressions are in Table-I, where

$$(n_1, n_2) = \begin{cases} (0, N - 1), & \text{for } j + l \leq N_g + \mu \\ (j + l - \mu - N_g, N - 1), & \text{for } l + j > N_g + \mu, \end{cases} \quad (21)$$

$$(n_3, n_4) = (0, j - \mu - N_g - 1), \quad (22)$$

Case f): $-\mu > N_g$. The expressions for this case are same as those of *Case e*), without the conditions on both j and $l + j$ and with

$$(n_1, n_2) = (j - \mu - N_g, N - 1), \quad (23)$$

$$(n_3, n_4) = (0, j + l - \mu - N_g - 1). \quad (24)$$

The expressions in W_2 in this case are same as those of *Case e*), without the conditions on both j and $l + j$ and with

$$(n_1, n_2) = (l + j - \mu - N_g, N - 1), \quad (25)$$

$$(n_3, n_4) = (0, j - \mu - N_g - 1). \quad (26)$$

A. Output SINR Expressions in W_1 and W_2

With the above characterization of the interference and desired signal terms for various cases of timing offset, we can obtain the average SINRs at the DFT output on the k th subcarrier in processing windows W_1 and W_2 . Denoting the average SINR in window W_n , $n = 1, 2$, as Γ_n , we can write

$$\Gamma_n = \frac{P_{DS}^n}{P_I^n + P_N^n}, \quad (27)$$

where P_{DS}^n , P_I^n and P_N^n are the average powers of the desired signal, interference, and noise, respectively, on k th subcarrier in window W_n . The expressions for P_I^1 and P_N^2 are given by

$$P_I^1 = \begin{cases} N_0 \left(1 + \frac{|\mu|}{N} + \frac{1}{LN} \left(\frac{|\mu|(L+|\mu|)}{2} \right) \right), & \text{for } |\mu| < L - 1 \\ N_0 \left(1 + \frac{|\mu|}{N} + \frac{1}{LN} \left(\frac{(L-2)(L-1)}{2} \right) \right), & \text{for } |\mu| \geq L - 1, \end{cases} \quad (28)$$

$$P_N^2 = \begin{cases} N_0 \left(2 + \frac{|\mu|}{N} - \frac{1}{LN} \left(\frac{|\mu|(L+|\mu|)}{2} \right) \right), & \text{for } |\mu| < L - 1 \\ N_0 \left(2 - \frac{|\mu|}{N} - \frac{1}{LN} \left(\frac{(L-2)(L-1)}{2} \right) \right), & \text{for } |\mu| \geq L - 1. \end{cases} \quad (29)$$

B. Numerical Results

We computed the average SINRs Γ_1 and Γ_2 using the expressions derived in the previous section. In Fig. 2, we plot the average SINR Γ_1 for $N = 64$, $L = 10$, $N_g = 18$, $G = 1$, as a function of the timing offset, μ , for different SNRs (5 dB, 10 dB, ∞). We have verified these analytically computed SINRs through simulations as well. Figure 2 shows that the SINR degrades significantly for large values of μ compared to $\mu = 0$ (i.e., perfect timing alignment), which is expected. It can be observed that, for a given magnitude of μ , the performance loss is more for $\mu > 0$ than for $\mu < 0$; e.g., with no

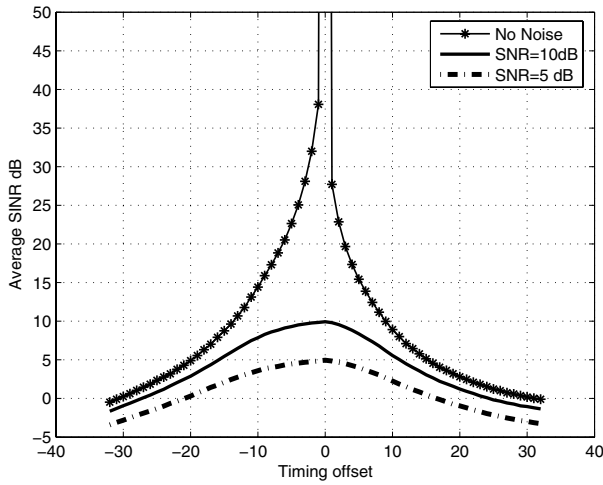


Fig. 2. Average SINR Γ_1 as a function of timing offset μ at the DFT output in cooperative OFDM with AF relaying. $N = 64$, $L = 10$, $N_g = 18$, SNR = 5 dB, 10 dB, ∞ (i.e., no noise).

noise, output SIR is about 38 dB for $\mu = -1$, and 28 dB for $\mu = 1$. This is because for $\mu < 0$, the interference increases without any reduction in the desired signal power in the frame arriving through the direct path because of the cyclic prefix, whereas for $\mu > 0$, the desired signal power get reduced in addition to the increase in interference power. Figure 1 highlights the possibility that interference mitigation techniques can alleviate the effect of large timing offsets in cooperative OFDM. Accordingly, in the following section, we present an interference cancelling receiver to alleviate the interference effects caused by large timing offsets.

IV. PROPOSED INTERFERENCE CANCELLER

Using an estimate of the next/previous and current frame interfering symbols and the channel fade coefficients, we can reconstruct the ISI terms which then can be subtracted from the received signal to achieve interference cancellation. To show how the IC works, consider *Case c*). The DFT-1 and DFT-2 outputs are of the form

$$Y_d[k] = X[k]\mathcal{H}_d[k] + \sum_{\substack{q=0 \\ q \neq k}}^{N-1} Y_{d,q}^{CFI}(X[q]) + \sum_{q=0}^{N-1} Y_{d,q}^{PFI}(X_p[q]) + Z_d[k], \quad (30)$$

$$Y_r[k] = X[k]\mathcal{H}_r[k] + \sum_{\substack{q=0 \\ q \neq k}}^{N-1} Y_{d,q}^{CFI}(X[q]) + Z_r[k], \quad (31)$$

where $Y_{d,q}^{CFI}(X[q])$ and $Y_{r,q}^{CFI}(X[q])$ are the ISI-CF terms due to q th carrier in the present frame, and $Y_{d,q}^{PFI}(X_p[q])$ is the ISI-PF term due to q th carrier in the previous frame, and $\mathcal{H}_d[k]$ and $\mathcal{H}_r[k]$ are the effective frequency responses of direct path and the path through the relay, respectively. In the first stage of the IC, all the symbols in the current frame are detected using

$$\hat{X}^1[k] = \text{sgn}(\Re(Y_d[k]\mathcal{H}_d^*[k] + Y_r[k]\mathcal{H}_r^*[k])), \quad (32)$$

where $\mathcal{H}_d^*[k]$ and $\mathcal{H}_r^*[k]$ are the complex conjugates of $\mathcal{H}_d[k]$ and $\mathcal{H}_r[k]$, respectively. In the m th stage of the interference canceler for $m \geq 2$, the symbols are detected using

$$\hat{X}^m[k] = \text{sgn}(\Re(Y_d^m[k]\mathcal{H}_d^*[k] + Y_r^m[k]\mathcal{H}_r^*[k])), \quad (33)$$

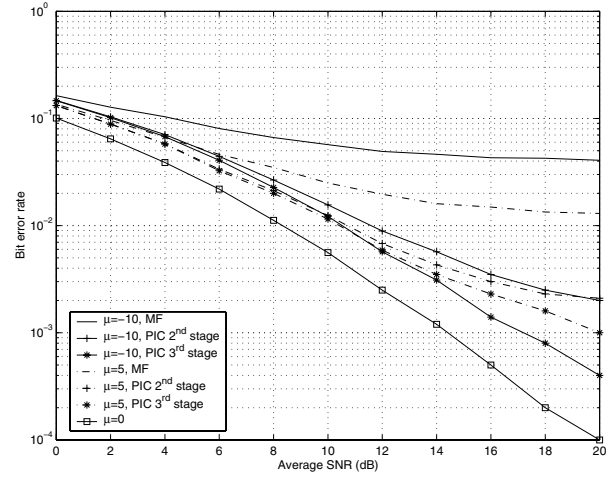


Fig. 3. BER performance of the interference canceler as a function of SNR for different values timing offsets, $\mu = -10, 5, 0$, in cooperative OFDM with AF relaying. $N = 64$, $L = 2$, $N_g = 2$, BPSK.

where $Y_d^m[k]$ and $Y_r^m[k]$ are the interference canceled DFT outputs, given by

$$Y_d^m[k] = X[k]\mathcal{H}_d[k] + \sum_{\substack{q=0 \\ q \neq k}}^{N-1} Y_{d,q}^{CFI}(X[q] - \hat{X}^{m-1}[q]) + \sum_{q=0}^{N-1} Y_{d,q}^{PFI}(X_p[q] - \hat{X}_p[q]) + Z_d[k],$$

$$Y_r^m[k] = X[k]\mathcal{H}_r[k] + \sum_{\substack{q=0 \\ q \neq k}}^{N-1} Y_{d,q}^{CFI}(X[q] - \hat{X}^{m-1}[q]) + Z_r[k],$$

where \hat{X}^{m-1} are the present frame symbols detected in the previous stage and $\hat{X}_p[q]$ are the symbols of the previous frame finally detected.

In Fig. 3, we present the simulated BER performance of the proposed interference canceler as a function of SNR, for a cooperative OFDM system with $N = 64$, $L = 2$, $N_g = 2$, BPSK, for different values of timing offsets, $\mu = -10, 5$. The BER performance in the case of perfect timing alignment, i.e., $\mu = 0$, is also plotted for comparison. Performance for different stages (i.e., $m = 2, 3$) of the proposed canceler are plotted. It can be seen that when $\mu = -10$ and 5, without interference cancellation (i.e., $m = 1$, which is the MF detector) the BER degrades significantly causing a high error floor. However, with the 2nd and 3rd stages of the proposed interference canceler, the BER improves significantly getting closer to the perfect timing performance. For example, the BER is 4×10^{-2} without cancellation for $\mu = -10$ at SNR=20 dB, and this BER improves to 2×10^{-3} with one stage of cancellation ($m = 2$), and it further improves to 4×10^{-4} with two stages of cancellation ($m = 3$), establishing the effectiveness of the proposed cancellation approach.

V. CONCLUSION

We investigated the effect of imperfect time alignment at the receiver in cooperative OFDM networks using amplify-and-forward protocol. We derived expressions for the average SINR at the DFT output, and quantified the degradation in the average SINR as a function of the timing offset. As a means to alleviate the interference effects caused by timing offsets, we presented an interference cancelling receiver and

Case	Window	DFT output on k th subcarrier	Term	Average power
a)	W ₁	$X[k]e^{\frac{i2\pi\mu k}{N}} \left(\sum_j h_d[j]e^{-\frac{i2\pi jk}{N}} \rho_{kk}(n_1, n_2) \right)$	DS	$\frac{1}{L} \sum_j \rho_{kk}(n_1, n_2) ^2$
		$+ \sum_{\substack{j,l \\ j+l < \mu}} G h_s[j] h_r[l] e^{-\frac{i2\pi(l+j+N_g)k}{N}} \rho_{kk}(n_3, n_4)$		
		$+ \sum_{\substack{q=0 \\ q \neq k}}^{N-1} X[q]e^{\frac{i2\pi\mu q}{N}} \left(\sum_{\substack{j \\ j \neq k}} h_d[j]e^{-\frac{i2\pi j q}{N}} \rho_{qk}(n_1, n_2) \right)$	ISI-CF	$\sum_{\substack{q=0 \\ q \neq k}}^{N-1} \left(\frac{1}{L} \sum_j \rho_{qk}(n_1, n_2) ^2 \right)$
	$+ \sum_{\substack{j,l \\ j+l < \mu}} G h_r[l] h_s[j] e^{-\frac{i2\pi(l+j+N_g)q}{N}} \rho_{qk}(n_3, n_4)$			
	W ₂	$GX[k]e^{\frac{i2\pi\mu k}{N}} \sum_{j,l} h_s[j] h_r[l] e^{-\frac{i2\pi(l+j)k}{N}} \rho_{kk}(n_1, n_2)$	DS	$(\frac{1}{L})^2 G^2 \sum_{j,l} \rho_{kk}(n_1, n_2) ^2$
$+ G \sum_{\substack{q=0 \\ q \neq k}}^{N-1} X[q]e^{\frac{i2\pi\mu q}{N}} \sum_{\substack{j,l \\ j+l < \mu}} h_s[j] h_r[l] e^{-\frac{i2\pi(l+j)q}{N}} \rho_{qk}(n_1, n_2)$		ISI-CF	$(\frac{1}{L})^2 G^2 \sum_{\substack{q=0 \\ q \neq k}}^{N-1} \sum_{\substack{j,l \\ j+l < \mu}} \rho_{qk}(n_1, n_2) ^2$	
$+ \sum_{q=0}^{N-1} X_f[q]e^{\frac{i2\pi(\mu-N_g)q}{N}} \sum_{j \leq \mu} h_{df}[j]e^{-\frac{i2\pi j q}{N}} \rho_{qk}(n_3, n_4)$		ISI-NF	$\sum_{q=0}^{N-1} \frac{1}{L} \sum_{j \leq \mu} \rho_{qk}(n_3, n_4) ^2$	
d)	W ₁	$X[k]e^{\frac{i2\pi\mu k}{N}} \sum_j h_d[j]e^{-\frac{i2\pi jk}{N}}$	DS	1
		$+ G \sum_{q=0}^{N-1} X_p[q] \left(e^{\frac{i2\pi\mu q}{N}} \sum_{\substack{j,l \\ j+l > N_g + \mu}} h_s p[j] h_r p[l] e^{-\frac{i2\pi(l+j-N_g)q}{N}} \rho_{qk}(n_1, n_2) \right)$	ISI-PF	$(\frac{1}{L})^2 \sum_{q=0}^{N-1} \sum_{\substack{j,l \\ j+l > N_g + \mu}} \left(G^2 \rho_{qk}(n_1, n_2) ^2 \right)$
	W ₂	$GX[k]e^{\frac{i2\pi\mu k}{N}} \sum_{j,l} h_s[j] h_r[l] e^{-\frac{i2\pi(l+j)k}{N}} \rho_{kk}(n_1, n_2)$	DS	$(\frac{1}{L})^2 G^2 \sum_{j,l} \rho_{kk}(n_1, n_2) ^2$
		$+ G \sum_{\substack{q=0 \\ q \neq k}}^{N-1} X[q]e^{\frac{i2\pi\mu q}{N}} \sum_{\substack{j,l \\ j+l < \mu}} h_s[j] h_r[l] e^{-\frac{i2\pi(l+j)q}{N}} \rho_{qk}(n_1, n_2)$	ISI-CF	$+(\frac{1}{L})^2 G^2 \sum_{\substack{q=0 \\ q \neq k}}^{N-1} \sum_{\substack{j,l \\ j+l < \mu}} \rho_{qk}(n_1, n_2) ^2$
e)	W ₁	$X[k]e^{\frac{i2\pi\mu k}{N}} \sum_j h_d[j]e^{-\frac{i2\pi jk}{N}} \rho_{kk}(n_1, n_2)$	DS	$\frac{1}{L} \sum_j \rho_{kk}(n_1, n_2) ^2$
		$+ \sum_{\substack{q=0 \\ q \neq k}}^{N-1} X[q]e^{\frac{i2\pi\mu q}{N}} \sum_j h_d[j]e^{-\frac{i2\pi j q}{N}} \rho_{qk}(n_1, n_2)$	ISI-CF	$\frac{1}{L} \sum_{\substack{q=0 \\ q \neq k}}^{N-1} \sum_j \rho_{qk}(n_1, n_2) ^2$
		$+ G \sum_{q=0}^{N-1} X_p[q] \left(e^{\frac{i2\pi\mu q}{N}} \sum_{\substack{j,l \\ j+l > N_g + \mu}} h_s p[j] h_r p[l] e^{-\frac{i2\pi(l+j-N_g)q}{N}} \rho_{qk}(n_3, n_4) \right)$	ISI-PF	$(\frac{1}{L})^2 G^2 \sum_{q=0}^{N-1} \left(\sum_{\substack{j,l \\ j+l > N_g + \mu}} \rho_{qk}(n_3, n_4) ^2 \right)$
	W ₂	$X[k]e^{\frac{i2\pi\mu k}{N}} \left(\sum_{j,l} G h_s[j] h_r[l] e^{-\frac{i2\pi(l+j)k}{N}} \rho_{kk}(n_1, n_2) \right)$	DS	$(\frac{1}{L})^2 G^2 \sum_{j,l} \rho_{kk}(n_1, n_2) ^2$
		$+ e^{\frac{i2\pi N_g k}{N}} \sum_{\substack{j \\ j > N_g + \mu}} h_d[j]e^{-\frac{i2\pi jk}{N}} \rho_{kk}(n_3, n_4)$		
		$\sum_{\substack{q=0 \\ q \neq k}}^{N-1} X[q]e^{\frac{i2\pi\mu q}{N}} \left(G \sum_{j,l} h_s[j] h_r[l] e^{-\frac{i2\pi(l+j)q}{N}} \rho_{qk}(n_1, n_2) \right)$	ISI-CF	$(\frac{1}{L})^2 G^2 \sum_{\substack{q=0 \\ q \neq k}}^{N-1} \rho_{qk}(n_1, n_2) ^2$
	$+ e^{\frac{i2\pi N_g q}{N}} \sum_{\substack{j \\ j > N_g + \mu}} h_d[j]e^{-\frac{i2\pi j q}{N}} \rho_{qk}(n_3, n_4)$	ISI-CF	$+\frac{1}{L} \sum_{\substack{q \neq k}}^{N-1} \sum_{\substack{j \\ j > N_g + \mu}} \rho_{qk}(n_3, n_4) ^2$	

TABLE I

showed that it provides improved bit error performance in the presence of large timing offsets.

REFERENCES

- [1] A. Nosratinia, E. Hunter, A. Hedayat, "Cooperative communication in wireless networks," *IEEE Commun. Mag.*, pp. 74-80, October 2004.
- [2] Y. (Geoffrey) Li and G. L. Stuber, *Orthogonal Frequency Division Multiplexing for Wireless Communications*, Springer, 2006.
- [3] B. Gui, L. J. Cimini, Jr., "Bit loading algorithms for cooperative OFDM systems," *EURASIP J. on Wireless Commun. and Networking*, vol. 2008, article ID 476797, 9 pages, 2008. doi:10.1155/2008/476797.
- [4] B. Gui, L. J. Cimini Jr., L. Dai, "OFDM for cooperative networking with limited channel state information," *IEEE MILCOM'06*, pp. 1-6, October 2006.
- [5] L. Dai, B. Gui, L. J. Cimini Jr., "Selective relaying in OFDM multihop cooperative networks," *IEEE WCNC'2007*, pp. 963-968, March 2007.
- [6] A. Jamshidi, M. Nasiri-Kenari, A. Taherpour, "Outage probability analysis of a coded cooperative OFDM system in multipath Rayleigh fading channels," *IEEE PIMRC'2007*, pages 1-6, September 2007.
- [7] X. Li, F. Ng, T. Han, "Carrier frequency offset mitigation in asynchronous cooperative OFDM transmissions," *IEEE Trans. Signal processing*, vol. 56, no. 2, 675-685, February 2008.
- [8] D. Sreedhar, A. Chockalingam, "Interference mitigation in cooperative SFBC-OFDM," *EURASIP J. on Advances in Sig. Proc.: Spl. Iss. on Wireless Cooperative Networks*, vol. 2008, article ID 125735, 11 pages, doi:10.1155/2008/125735.
- [9] Y. Mei, Y. Hua, A. Swami, and B. Daneshrad, "Combating synchronization errors in cooperative relays," *IEEE ICASSP'2005*, pp. 369-372, March 2005.
- [10] S. Wei, D. L. Goeckel, M. C. Valenti, "Asynchronous cooperative diversity," *IEEE Trans. Wireless Commun.*, pp. 1547-1557, June 2006.